Available online at www.sciencedirect.com
ScienceDirect
International Journal of Mass Spectrometry 272 (2008) 48–56
International Journal of Mass Spectrometry
www.elsevier.com/locate/ijms

Absolute partial cross-sections for the destruction of H_2 and H_3^+ in collisions with helium atoms at 50 and 60 keV/amu

J. Tabet, S. Eden, F. Gobet, B. Farizon *, M. Farizon, S. Ouaskit [1], P. Scheier [2], T.D. Märk [2]

Institut de Physique Nucléaire de Lyon, Université de Lyon, Université Claude Bernard Lyon I, IN2P3-CNRS 43, boulevard du 11 Novembre 1918, 69622 Villeurbanne Cedex, France

Received 19 July 2007; received in revised form 18 December 2007; accepted 19 December 2007
Available online 28 December 2007

Abstract

The first partial cross-section measurements are presented for the various channels of H_3^+ and H_2 dissociation in collisions with helium atoms at 50 and 60 keV/amu. The experimental technique includes the use of a removable grid in front of a surface barrier detector to enable neutrals of mass 2 amu to be separated into H_2 and 2H channels.

Keywords: Molecular hydrogen; H_2; H_3^+; Collision induced fragmentation; Ionization reference

1. Introduction

A significant number of experimental and theoretical studies have been carried out upon atomic collisions with the simplest molecules and molecular ions: H_2, H_2^+, and H_3^+. These interactions are of major interest both on a fundamental level as model systems for molecular fragmentation and ionization and in various areas of applied physics and chemistry. In particular, besides being a common ion in hydrogen discharges and plasmas, H_3^+ is understood to be abundant in the interstellar medium [1] where interactions with cosmic rays (including fast neutralized α particles) can have important effects on the chemistry and thermodynamics of interstellar clouds. Furthermore, the specific cross-sections presented in this article are valuable for the interpretation of the effects of cluster size upon the fragmentation of hydrogen cluster ions comprising a number of H_2 molecules surrounding an H_3^+ core, with implications relating to shell structures and temperature [2].

In the present energy range, a collision with a helium atom may induce two dominant processes in an H_3^+ molecular ion: electronic excitation (including ionization) and the capture of an electron from the target atom. Conversely, electron capture by an H_2 molecule in a collision with an atomic target is negligible. Following the interaction, the molecular H_2 system relaxes and may dissociate. The detection of both neutral and ionic fragments enables certain electronic excitation events which do not involve a change in the charge state of the projectile system to be identified. The total cross-section for H_3^+ dissociation in 60 keV/amu collisions with helium has been reported in a recent publication [2]. However, with the exceptions of this result and Bouliou et al.'s [3] measurement of H_2^+ production in H_2 collisions with He atoms at 50 keV/amu, the present communication provides the first cross-sections in the *intermediate* velocity range for the various total and partial ionization and dissociation channels observable with the present apparatus.

2. Experimental

The experiments were carried out using a crossed-beam apparatus, part of which is shown schematically in Fig. 1. Pure molecular hydrogen is ionized in a standard RF-discharge source (80 MHz). Typical parameters for the ion source are 30 W RF-power and an H_2 pressure of 10^{-3} Torr. The accelerator system

* Corresponding author.
E-mail address: bfarizon@ipnl.in2p3.fr (B. Farizon).
[1] Permanent address: Université Hassan II-Mohammédia, Faculté des Sciences Ben M'Sik (LPMC), B.P.7955 Ben M'Sik, Casablanca, Morocco.
[2] Institut für Ionenphysik und Angewandte Physik, Leopold Franzens Universität, Technikerstrasse 25, A-6020 Innsbruck, Austria.

1387-3806/$ – see front matter © 2008 Elsevier B.V. All rights reserved.
doi:10.1016/j.ijms.2007.12.014

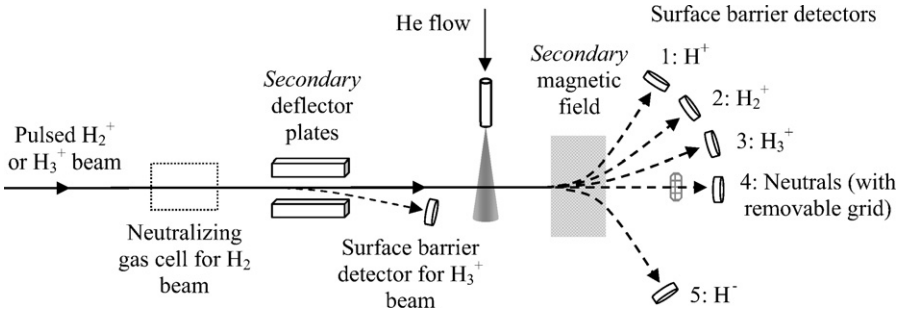

Fig. 1. Schematic diagram showing the experimental system around the collision region and the detector system.

(not shown in Fig. 1) has been described in detail by Carré et al. [4]. Briefly, a *primary* magnetic sector field is used to separate H_2^+ or H_3^+ from protons and other ions such as those originating from impurities in the source. The ion beam is pulsed by application of a voltage across *primary* parallel deflector plates (not shown in Fig. 1) situated before the primary magnetic field. After collimation using two circular apertures of radius 0.5 mm and set 1 m apart (also not shown in Fig. 1), the projectile beam is crossed at right angles with an effusive beam of helium gas. By means of a differential pumping system, the residual gas pressure close to the target jet and along the beamline is maintained at 10^{-6} Torr.

In order to measure the intensity of the incident H_3^+ beam and thereby subtract the contributions of any projectiles which have been neutralized by the residual gas, a voltage can be applied across *secondary* parallel deflector plates situated *upstream* from the target jet (see Fig. 1). By coinciding the voltage with alternate H_3^+ pulses, the projectile beam is directed to a surface barrier detector or continues to the collision chamber. In order to carry out the H_2 projectile experiments, neon is introduced into a charge transfer cell (path length 80 mm) between the primary magnetic sector field and the target jet. In this case, a potential is applied across the secondary deflector plates to eliminate residual charged projectiles. This also acts as a quenching field (10 kV cm^{-1}) for metastable molecules and as an ionizing field for Rydberg molecules [5]. The number of incident H_2 projectiles is derived from the molecules, ions, and neutrals observed at the surface barrier detectors after the collision chamber (numbered 1–5 in Fig. 1).

The helium target gas is introduced into the collision chamber via a capillary tube. A detailed description of the target jet and the absolute calibration technique is given by Ouaskit et al. [6]. The capillary tube is mounted on a micrometric gonimeter which enables the jet to be moved in all directions (X, Y, Z) in steps of 50 μm. The target width (€) of the jet depends upon the inlet pressure and the position of the capillary with respect to the incident beam. These parameters are measured to a minimum precision of 0.3% and 4%, respectively. In order to confirm that single collision conditions apply, the measured branching ratios are verified to be independent of changes in the target width.

The main features of the ion and neutral particle detection system have been described in previous publications related to H_n^+ cluster dissociation experiments [7]. Briefly, the transmitted beam is analyzed in a *secondary* magnetic field (shown in Fig. 1) located 1.5 m after the target, corresponding to respective flight times of 0.48 and 0.44 μs for 50 and 60 keV/amu projectiles. Barrier surface detectors (labeled 1–5 in Fig. 1) are mounted at the appropriate positions to detect H^+, H_2^+, H_3^+, neutrals, and H^- fragments on an event-by-event basis. The amplitude of the current impulse emitted by a surface barrier detector following ion or neutral impact is proportional to the energy deposited. Thus a single H atom arriving at surface barrier detector 4 (see Fig. 1) can be distinguished readily from an H_2 molecule, whereas the simultaneous arrival of two H atoms produces an indistinguishable signal to that of a single H_2 molecule. Indeed it is a challenge to observe non-ionizing dissociation of H_2 ($\rightarrow$2H) and to separate the H_3^+ electron capture channels leading to the formation of 3H and H_2 + H. For this purpose, a movable transmission grid was placed in front of the neutral detector (labeled 4 in Fig. 1) for H_2 and H_3^+ impact at 50 keV/amu and for H_2 impact at 60 keV/amu. Previous applications of grid transmission techniques for the separation of neutral production channels include the experiments carried out by Morgan et al. [8] and by Mitchell et al. [9]. The following explanation utilizes the example of observing H_2 non-ionizing dissociation. Branching ratios defined with (G) and without (S) the grid in front of the neutral detector are calculated as the number of neutrals detected of 2 amu, N(*2 amu Neutral*), divided by the number of events corresponding to non-dissociative ionization, N(H_2^+), i.e.

$$G = \left(\frac{N(2\,\text{amu Neutral})}{N(H_2^+)}\right)_{\text{WITH GRID}} \quad (1a)$$

$$S = \left(\frac{N(2\,\text{amu Neutral})}{N(H_2^+)}\right)_{\text{WITHOUT GRID}} \quad (1b)$$

Naturally, $N(H_2^+)$ is independent of the position of the grid. The transmission, T, of the grid was measured optically to be 0.510 ± 0.007. Measurements of the $H_3^+ \rightarrow H_2^+ + H$ channel with and without the grid showed the transmission probability for hydrogen atoms to be 0.515 ± 0.015, within the error margins of the optical result. Kinetic energy release in the dissociation allied to the large distance from collision to detection (1.5 m) in comparison with the width of the holes in the grid (250 μm) enables the transmission of each neutral formed in a given dissociation to be considered independently. Therefore the probability for two neutrals formed in a single collision to pass through the grid is T^2. The proportion of N(*2 amu Neutral*) corresponding to the simultaneous arrival of 2 H atoms is defined as X and that

to the arrival of an H_2 molecule as $(1 - X)$. Accordingly we can derive the equations below.

$$G = \frac{T\,N(H_2) + T^2 N(2H)}{N(H_2{}^+)} \tag{2a}$$

$$= \frac{(T(1-X) + T^2 X)N(2\,\text{amu Neutral})}{N(H_2{}^+)} \tag{2b}$$

$$= (T(1-X) + T^2 X)S \tag{2c}$$

$$\rightarrow X = \frac{(G/S) - T}{T^2 - T} \tag{2d}$$

Thus branching ratios and cross-sections were deduced for the five channels listed below.

$$H_3{}^+ \rightarrow H^+ + H_2 \tag{3a}$$

$$H_3{}^+ \rightarrow H^+ + 2H \tag{3b}$$

$$H_3{}^+ \rightarrow H + H_2 \tag{3c}$$

$$H_3{}^+ \rightarrow H + 2H \tag{3d}$$

$$H_2 \rightarrow 2H \tag{3e}$$

Application of this technique without a helium target enabled us to determine the purity of the incident H_2 beam at 50 and 60 keV/amu to be 99%. The errors on branching ratios and absolute cross-sections not involving the distinction of the different $3N$ and $2N$ channels are estimated at ±5% and ±15%, respectively, on the basis of the maximum deviation of measurements repeated for different preparations of the experimental system. However, greater statistical errors apply to the branching ratios (estimated at ±20%) and cross-sections (±30%) for very weak channels, notably those involving H^- production. The branching ratios and partial cross-sections for H_2, 2H, 3H, and $H_2 + H$ channels are also subject to larger errors, respectively estimated at ±10% and ±20%, due to the additional measurement required using the grid (G in Eqs. (1a), (1b) and Eqs. (1) and (2)) and propagation of the error on the grid transmission (T).

Although the vibrational distribution within the present beams has not been measured, a significant proportion of the $H_3{}^+$ and H_2 projectiles are expected to be in rovibrationally excited states (average internal energies of the order 1–2 eV: see, for example, the works of Wolff et al. [10] and Peart and Dolder [11] for analogies). Bouliou et al. [3] commented that the good agreement between independently measured absolute cross-sections indicates that rovibrational excitation in the incident beam does not have a major effect on $H_2{}^+$ and H_2 fragmentation in 5–50 keV/amu collisions with atoms. Similarly, the good repeatability of our data and their apparent consistency of with the available measurements in the literature imply that the effects of rovibrational excitation in the incident beam on the present $H_3{}^+$ and H_2 fragmentation cross-sections are small in comparison with the experimental errors.

3. Results and discussion

3.1. $H_3{}^+$ collisions with helium atoms

The total destruction (dissociation and/or change of charge state) cross-section σ_{TD} for $H_3{}^+$ ions in a beam traversing a target jet of width € (the number of He atoms per unit area at the projectile beam intersection) is calculated using the equation below.

$$\sigma_{TD} = \ln\left(\frac{N_I}{N}\right)€^{-1} \tag{4}$$

Where N_I is the number of incident $H_3{}^+$ ions and N is the number of particles detected at the detector labeled 3 in Fig. 1. The target width is kept low to ensure that single collision conditions apply ($\sigma_{TD}€ \ll 1$). The total destruction cross-sections of $H_3{}^+$ given in Table 1 have been derived from measurements carried out with various different target widths and used to calculate the partial cross-sections on the basis of the measured branching ratios. It should be noted that σ_{TD} is not generated by summing the partial cross-sections for the various observed channels. This is more important in the case of the 60 keV/amu measurements which were carried out without detector 5 to observe H^- channels (0.14% of the dissociation events at 50 keV/amu). No attempt was made to observe channels including the exotic metastable fragments $H_2{}^-$ and $H_3{}^-$ due to previous experimental and theoretical studies supporting their non-existence [12,13]. However, readers should be aware that more recent measurements have demonstrated mechanisms of the production of both these molecular anions with minimum lifetimes of several μs [14]. It should also be noted the 60 keV/amu total destruction cross-section has been re-measured for a number of separate preparations of the experimental system, giving the averaged value $2.77 \times 10^{-17}\,cm^2$ with a reduced error of $\pm 0.17 \times 10^{-17}\,cm^2$ [2]. Accordingly, the errors on the partial cross-sections calculated using this result are estimated at ±10% instead of 15% (see Table 1).

No $H_3{}^+ \rightarrow H_3$ events were observed at 50 keV/amu. This is perhaps surprising as Gaillard et al. [15] reported the existence of H_3 states produced in $H_3{}^+$–argon atom collisions at 133–1000 keV/amu with lifetimes ≥0.3 μs, close to the present flight time of the projectile system from the helium jet to the detectors. By contrast, however, the mean lifetime of H_3 produced in 15 keV $H_3{}^+$ collisions with cesium atoms has been determined by Bruckmeier et al. [16] to be 3.9 ns. Similarly, Datz et al. [17] observed no H_3* products of free electron attachment to vibrationally de-excited $H_3{}^+$ at a detector situated ∼100 ns downstream from the interaction. The grid was not used in the present 60 keV/amu $H_3{}^+$ collision experiments so the different $3N$ channels could not be separated. By analogy with the 50 keV/amu results, the $H_3{}^+$ dissociation cross-section at 60 keV/amu is assumed to be equal to the measured total destruction cross-section to within the present statistical limits.

To the authors' knowledge, the only independent absolute destruction cross-sections which are comparable with the present data are those measured by Wolff et al. [10] for $H_3{}^+$ collisions with a helium target at energies ranging from 160

Table 1
Dissociation of H_3^+ in 50 keV/amu and 60 keV/amu collisions with helium atoms

Channel	50 keV / amu		60 keV / amu	
	Branching ratio ± 5 % [†] (σ / σ_{TD})	Cross section ± 15 % [†] (cm^2)	Branching ratio ± 5 % (σ / σ_{TD})	Cross section ± 10 % [†] (cm^2)
Total destruction (σ_{TD}) [‡]	-	3.35×10^{-16}	-	$(2.77 \pm 0.17) \times 10^{-16}$
3N *	0.27	9.0×10^{-17}	0.27	7.4×10^{-17}
$H + H^+ + H^-$	$(5.2 \pm 1.0) \times 10^{-4}$	$(1.7 \pm 0.5) \times 10^{-19}$	-	-
$H_2^+ + H^-$	$(2.7 \pm 0.5) \times 10^{-4}$	$(9.0 \pm 2.7) \times 10^{-20}$	-	-
$2N + H^-$	$(4.1 \pm 0.8) \times 10^{-4}$	$(1.4 \pm 0.4) \times 10^{-19}$	-	-
$2N + H^+$ *	0.18	6.2×10^{-17}	0.17	4.8×10^{-17}
$H_2^+ + H$	0.12	3.9×10^{-17}	0.12	3.4×10^{-17}
$2H^+ + H^-$	$(2.5 \pm 0.5) \times 10^{-4}$	$(8.4 \pm 2.5) \times 10^{-20}$	-	-
$H + 2H^+$	0.23	7.7×10^{-17}	0.21	5.8×10^{-17}
$H_2^+ + H^+$	0.14	4.7×10^{-17}	0.16	4.3×10^{-17}
$3H^+$	0.061	2.0×10^{-17}	0.072	2.0×10^{-17}
Sum (electron loss)	0.43	1.4×10^{-16}	0.44	1.2×10^{-16}
Sum (H^- production)	$(1.5 \pm 0.3) \times 10^{-3}$	$(4.9 \pm 1.5) \times 10^{-19}$	-	-
Sum (1N production) * °	0.35	1.2×10^{-16}	0.33	9.2×10^{-17}
Sum (2N production) *	0.18	6.2×10^{-17}	0.17	4.8×10^{-17}
Sum (H^+ channels)	0.62	2.1×10^{-16}	0.61	1.7×10^{-16}
Sum (H^+ production) [#]	-	3.2×10^{-16}	-	2.7×10^{-16}
Sum (H_2^+ production)	0.26	8.6×10^{-17}	0.28	7.7×10^{-17}

Shaded boxes contain branching ratios and cross-sections which were generated by summing distinct channels. The 60 keV/amu measurements are made without a detector for H^- fragments. However, on the basis of comparisons with the 50 keV/amu results, H^- channels are expected to contribute minimally to the 60 keV/amu sums given. [a]Unless errors are specified otherwise. [b]Assumed to be equal to total dissociation to within the present statistical limits as no H_3 molecules are observed (see text). [c]3*N* and 2*N* signify the detection of neutrals of total mass 3 or 2 amu, respectively, i.e., possible combinations of H atoms and H_2 molecules. [d]H detection without the possible simultaneous arrival of an H_2 molecule or another H atom (or another 2 H atoms). [e]This cross-section can be compared directly with current-type measurement; the cross-sections for channels including the production of two or 3 H^+ ions are respectively counted twice or three times for the sum.

to 1230 keV/amu. Wolff et al. [10] demonstrated an approximately linear dependence of $(\sigma_{TD})^{-1}$ upon the square of the impact velocity in collisions with Ne, Ar, Xe, and He. This relation is associated with Meron and Johnson's [18] model for electron loss in atomic systems (discussed further in Section 3.2). Fig. 2 shows that the present 50 and 60 keV/amu electron-loss cross-sections are broadly consistent with this relation, lying close to the lower error boundary of the extrapolated $(\sigma_{TD})^{-1} = a + bv^2$ weighted fit (Origin Pro™ Version 7) to the previous total destruction cross-sections [10]. Whereas electron-loss is expected to dominate H_3^+ destruction at the impact energies studied by Wolff et al. [10], Table 1 shows that less than 50% of the observed H_3^+ destruction events involve electron loss for collisions with helium atoms at 50 and 60 keV/amu.

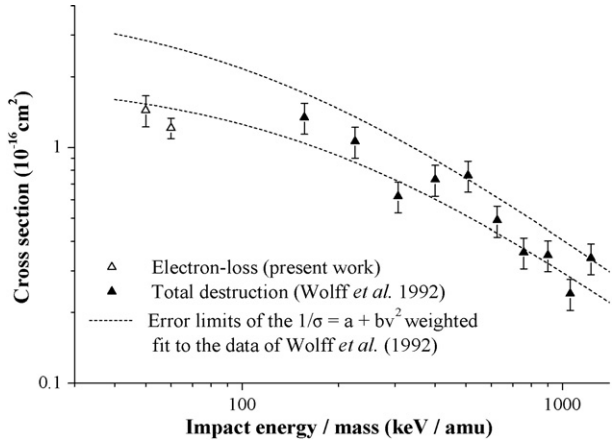

Fig. 2. Comparison of the present cross-sections for electron-loss from H_3^+ with the total destruction cross-sections of Wolff et al. [10] for higher energy H_3^+ collisions with helium atoms.

A number of studies have been carried out on the production of H^- ions in H_3^+ dissociation events [19–25]. These ions can be produced either by H_3 dissociation following electron capture or by electronic excitation (including ionization) of H_3^+. As the present experiments include neither the detection of emitted electrons nor the measurement of the post-collision charge state of the helium target, it is not possible to determine the proportion of electron capture events within most observed channels. Only for channels with more than two bound electrons on the detected fragments can electron capture be unambiguously identified. Electron capture processes are naturally expected to lead to higher H^- production rates as there are more electrons in the excited projectile system. Accordingly, H^- production channels represent 0.44% of the presently identifiable electron capture events (3*N*, $H + H^+ + H^-$, $H_2^+ + H^-$, and $2N + H^-$) at 50 keV/amu compared to 0.034% of the other observed destruction events (presumably dominated by electronic excitation), while the major channel for H^- production is $(H + H^+ + H^-)$. From a theoretical point of view, this channel is particularly interesting for the study of a three-body system in the presence of Coulomb interactions.

Yenen et al. [23] measured the energy distribution of H^- produced in H_3^+ collisions with helium atoms in the energy range 0.8–2.3 keV/amu and concluded that the detected H^- fragments were formed by the electronic excitation of H_3^+ followed by its fragmentation ($\rightarrow 2H^+ + H^-$). However, the present 50 keV/amu measurements show that over 80% of the observed H^- ions are produced in identified electron capture processes. This suggests a distinct change in the dominant production process for H^- ions between collisions at low ($\sim 0.3\ v_0$) and intermediate ($\sim 1.4\ v_0$) velocities. Absolute cross-section measurements for total H^- production in H_3^+ collisions with

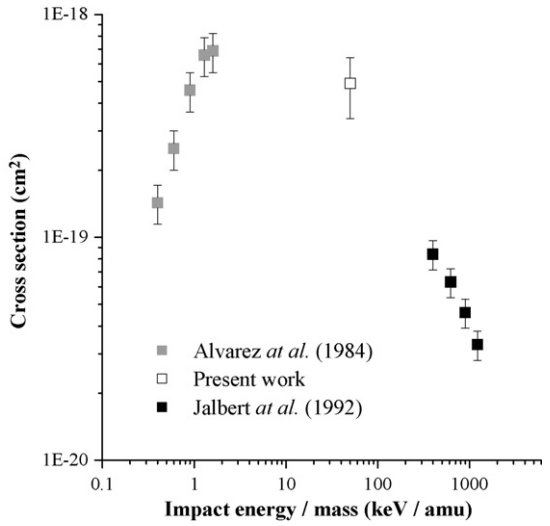

Fig. 3. Comparisons of the present partial cross-sections for H^- production in H_3^+ collisions with helium atoms with previous measurements at different impact energies [20,22].

helium atoms have been reported by Alvarez et al. [22] and Jalbert et al. [20] in the respective energy ranges 0.4–1.6 and 400–1200 keV/amu. Fig. 3 suggests a broad consistency of the present 50 keV/amu total H^- production cross-section with the previous results.

The present partial cross-sections for H^+ and H_2^+ production are plotted in Fig. 4 together with the previous measurements carried out at lower collision energies. In order to make a direct comparison with the current-type measurements of Williams and Dunbar [26], the present $2H^+$ and $3H^+$ channels are, respectively, counted twice and three times to calculate the summed cross-section for H^+ production shown in the figure. The present data appear to be consistent with a continuation up to 50 and

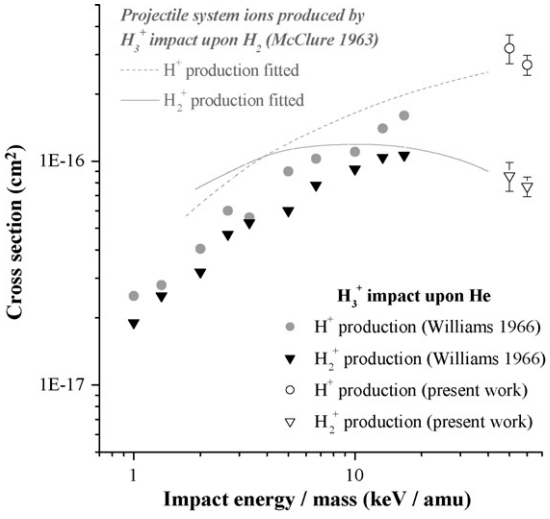

Fig. 4. Comparisons of the present partial cross-sections for H^+ and H_2^+ (open circles and triangles) production in H_3^+ collisions with helium atoms with previous measurements at lower impact energies (filled circles and triangles) [26]. The lines shown in the figure represent McClure's [27] cross-section measurements for the formation of H^+ and H_2^+ ions by dissociation of the projectile system following H_3^+ impact upon H_2 molecules.

60 keV/amu of the trend observed by Williams and Dunbar [26] for gradual increase in H^+ production with impact energy in the range 1–17 keV/amu. This trend is also visible in McClure et al.'s [27] cross-sections for the formation of H^+ ions by dissociation of the projectile system following H_3^+ impact upon H_2 molecules at 2–40 keV/amu (represented as a solid line in Fig. 4). It is interesting to note the seemingly good agreement of the present and past helium impact absolute cross-sections with the H_2 target results of McClure et al. [27]. This appears to be consistent with Wolff et al.'s [10] observation at higher impact velocities of an empirical 4th order dependence of total H_3^+ destruction cross-section upon the geometrical radius of the atomic target, and Mais' [28] determination that the effective collision radius of H_2 is less than 5% greater than that of He in a low-velocity K atom scattering experiment. By contrast, the considerably higher ground-state ionization energy of He (24.6 eV compared to 15.4 eV [29]) indicates that He and H_2 do not have similar electron velocities, generally considered to be an important parameter for electron capture by a charged projectile.

As is the case for H^+, the only previous H_2^+ production cross-sections for H_3^+ impact upon atomic helium were reported by Williams and Dunbar [26] at lower energies. The distribution of present and previous measurements for H_3^+ impact upon He shown in Fig. 4 suggests a maximum in H_2^+ production between 20 and 30 keV/amu. McClure et al.'s [27] cross-sections for the formation of H_2^+ ions by dissociation of the projectile system following H_3^+ impact upon an H_2 target (represented as a solid line in the figure) show similar characteristics with a maximum around 10 keV/amu. It is interesting to note that the present cross-section for H_2^+ production is less than 30% of that for H^+ production, much lower than the average value of 80% in 1–17 keV/amu collisions with He atoms [26]. This suggests a possible increase in the branching ratio for three-body dissociation (the only channels which can yield more than one H^+) at 50 and 60 keV/amu compared to 1–17 keV/amu. Indeed, two body dissociation accounts for only 18% of total number of H^+ ions detected following 50 keV/amu collisions.

Cross-sections for the production of neutrals in H_3^+ collisions with helium atoms have been reported by Jalbert et al. [30] in the energy range 400–1200 keV/amu. The present cross-sections for $1N$ production, corresponding to H detection without the simultaneous detection of an H_2 molecule or one or two other H atoms, and $2N$ production (2 H atoms or an H_2 molecule) are compared to the previous data [30] in Fig. 5. The present data at 50 and 60 keV/amu appear to be consistent with the broad trend for decreasing $1N$ and $2N$ production with increasing impact energy observed between 400 and 1200 keV/amu [30] and with Mclure's [27] observation of a maximum at around 10 keV/amu for the formation of neutral fragments by dissociation of the projectile system following H_3^+ impact upon an H_2 target. It is also worth noting that the present $2N$ production cross-sections are around one half of the $1N$ cross-sections, while the data of Jalbert et al. [30] in the range 400–1200 keV/amu show $2N$ production to be lower as a proportion of $1N$ production. This suggests that electron capture processes, whose probability can be assumed to fall rapidly with energy above ~100 keV/amu,

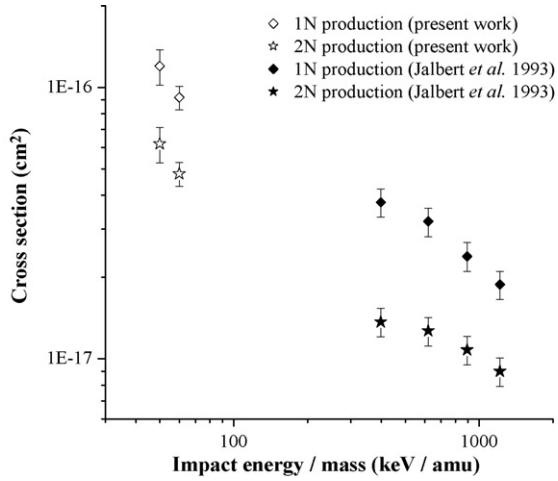

Fig. 5. Comparisons of the present partial cross-sections for 1*N* (H without simultaneous detection of an H_2 or another H) and 2*N* (H_2 or 2H) production in H_3^+ collisions with helium atoms with previous measurements at different impact energies [30].

may have a particularly significant contribution to the presently observed 2*N* channels. Table 2 shows that H_2 production (two body dissociation) at 50 keV/amu represents 80% of the 2*N* events.

To the authors' knowledge, no previous absolute cross-sections have been reported for the H_3^+ dissociation channels listed in Table 2 for 50 keV/amu (1.4 v_0) collisions with helium atoms. However, it is interesting to compare the present branching ratios for 3*N* production (exclusively due to electron capture) with those measured by Datz et al. [17] for H_3^+ dissociation following the capture of a free electron in the energy range 0.001–20 eV (0.01–1.2 v_0). Datz et al. [17] reported that (H_2 + H) production remained constant at ~25% of the total 3*N* dissociation events from 0.001 to 0.4 eV, and then increased to a maximum of ~65% close to 4 eV. Above 4 eV, the measured proportion of (H_2 + H) events steadily decreased to ~10% at 20 eV. An interpretation for this energy dependence was proposed in terms of inelastic interactions between the electron and the H_3^+ ion [17]. In the present work, the H_2 + H channel represents 89% of the 3*N* detection events, markedly higher than Datz et al.'s [17] observations. The distinct difference between the relative contributions of the 3H and (H_2 + H) channels observed in H_3^+ interactions with a helium atom and with a free electron suggests that the He target plays more than a simple *spectator* role in dissociative electron capture processes.

It is interesting to consider the present 3H/(H_2 + H) branching ratio of 0.11 ± 0.02 for 50 keV/amu H_3^+ impact upon helium atoms in the context of Peterson et al.'s [31] results for *near-resonant* (little change in internal energy) electron capture in 1 keV/amu (0.2 v_0) H_3^+ collisions with Cs atoms. In particular, Peterson et al. [31] reported that more highly excited incident H_3^+ yielded higher 3H/(H_2 + H) branching ratios (0.23 ± 0.02 and 0.65 ± 0.02 for respective average H_3* internal energies of 1.48 ± 0.15 and 2.42 ± 0.2 eV). However, the much lower impact parameters for electron capture in the present collisions are associated with significant energy transfer (non-resonant conditions). This energy transfer is expected to reduce the relative importance of the internal energy of the incident molecular ions, in accordance with Wolff et al.'s [10] argument relating to 160–1230 keV/amu H_3^+–He collisions.

No clear evidence is observed for energy dependence between the 50 and 60 keV/amu cross-sections (total, partial, or summed). Although the total H_3^+ destruction cross-section is 18% greater at 50 keV/amu, this may be accounted for by the combination of ±15% errors. Table 1 demonstrates the present branching ratios to be in exceptionally good agreement. That the branching ratios are similar is not surprising as the energies are sufficiently close to expect the same types of interactions to dominate. Only the $3H^+$ channel shows evidence for branching ratio dependence upon impact energy in the present range. It may be envisaged that this channel occurs preferentially in high-energy collisions as it represents a maximum *break up* of the protons and electrons which make up the H_3^+ projectile. However, it should also be noted that the branching ratio errors are essentially statistical and thus a relatively large error can be expected for the $3H^+$ channel, the weakest of those which are observed at both 50 and 60 keV/amu.

3.2. H_2 collisions with helium atoms

The present total cross-sections $\sigma_d(H_2)$ for the destruction (dissociation and/or ionization) of H_2 by helium impact

Table 2
Separation of 2H from H_2 detection in H_3^+ dissociation at 50 keV/amu collisions with helium atoms

Channel	Branching ratio ± 10 % [†] (σ / σ_{TD})	Cross section ± 20 % [†] (cm^2)
3H	0.028	9.4×10^{-18}
H_2 + H	0.24	8.0×10^{-17}
$H_2 + H^+$	0.035	1.2×10^{-17}
$2H + H^+$	0.15	5.0×10^{-17}
Sum (H channels)*	0.76 ± 0.05	$(2.6 \pm 0.4) \times 10^{-16}$
Sum (H production)* [#]	-	$(3.2 \pm 0.6) \times 10^{-16}$
Sum (H_2 production)	0.28	9.2×10^{-17}
Sum (2 body dissociation)*	0.53 ± 0.05	$(1.8 \pm 0.3) \times 10^{-16}$
Sum (3 body dissociation)*	0.47 ± 0.04	$(1.6 \pm 0.3) \times 10^{-17}$

Shaded boxes contain branching ratios and cross-sections which were generated by summing distinct channels. The partial cross-section for $2N + H^-$ is too low to accumulate sufficient statistics to carry out a meaningful separation of H_2 and 2H channels. [a]Unless errors are specified otherwise. [b]These sums include partial cross-sections from Table 1. [c]This cross-section can be compared directly with a current-type measurement, i.e., the cross-sections for channels including the production of two H atoms are counted twice for the sum.

are $(3.1 \pm 0.5) \times 10^{-16}$ and $(3.2 \pm 0.5) \times 10^{-16}$ cm^2 at 50 and 60 keV/amu, respectively. These cross-sections are generated by summing the partial cross-sections listed in Table 3. Very few studies of H_2 excitation by atomic or molecular impact have been carried out [3,32,33], while the particular rarity of total cross-section measurements for dissociation and destruction is largely due to the difficulty in identifying neutral dissociation events ($H_2 \rightarrow 2H$). Indeed, to the authors' knowledge, the present work provides the first experimental cross-sections and branching ratios for neutral dissociation of H_2 in collisions with any atomic or molecular target.

De Castro Faria et al. [34] reported cross-sections for H_2 destruction based on attenuation measurements of a neutral molecular beam in a magnetic field following 225–1220 keV/amu collisions with helium atoms, thus assuming neutral dissociation to be negligible. It was inferred that H_2 destruction in this energy range proceeds dominantly through ionization as opposed to through H_2 excitation on the basis of comparisons with a Bohr-type model in which molecular cross-sections are inversely proportional to the dissociation energy [34,35]. This model fits the data much better when the H_2 dissociation energy is taken to be 16.3 eV, the ionization energy, rather than 10.0 eV, the excitation energy for the first dissociative state ($b^3\Sigma_u^+$). The present work shows that ionization channels account for 86% and 84% of the observed H_2 destruction events at 50 and 60 keV/amu, respectively (Table 3). Therefore, while ionization dominates H_2 destruction, neutral dissociation is not negligible at the present impact energies.

As reported by the same group for H_3^+ collisions with a helium target [10], de Castro Faria et al. [34] demonstrated an approximately linear dependence of the reciprocal of the H_2 destruction cross-section (not including neutral dissociation) upon the square of the impact velocity in collisions with Ne, Ar, and He, in accordance with the free-collision model (FCM) of Meron and Johnson [18] for electron loss in atomic systems. In order to make a direct comparison with the results of de Castro Faria et al. [34], the present cross-sections for H_2 electron loss ($\sigma_{EL} \approx$ destruction with neutral dissociation removed) are plotted in Fig. 6. Although the present cross-sections lie outside the error boundaries of the extrapolated $(\sigma_{EL})^{-1} = a + bv^2$ weighted fit (Origin Pro^{TM} Version 7) to the data of de Castro Faria et al. [34], the two sets of results do not appear to be markedly inconsistent.

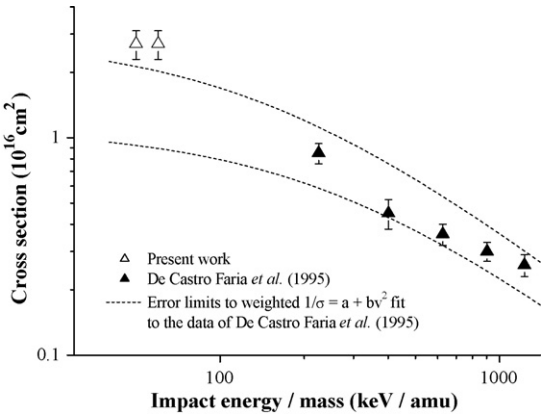

Fig. 6. Comparisons of the present total H_2 electron loss cross-sections with the previous data [34] for higher energy collisions with helium atoms.

While, to the authors' knowledge, no total destruction cross-sections are available for H_2 impact upon a helium target, cross-sections for collisions between two H_2 molecules have been calculated analytically on the basis experimental viscosity data and H^+ projectile data scaled using a coefficient derived from screened Coulomb theory [32,33]. As discussed in Section 3.1, dihydrogen molecules have been observed to display similar cross-sections to helium atoms (see Fig. 4). Accordingly the present total H_2 destruction cross-section for 50 keV/amu He impact $(3.1 \pm 0.5) \times 10^{-16}$ cm^2, is in agreement with the cross-

Table 3
Dissociation of H_2 in 50 and 60 keV/amu collisions with helium atoms

Channel	50 keV / amu		60 keV / amu	
	Branching ratio ± 5 % [†] (σ / σ$_{TD}$)	Cross section ± 15 % [†] (cm^2)	Branching ratio ± 5 % [†] (σ / σ$_{TD}$)	Cross section ± 15 % [†] (cm^2)
$H^- + H$	$(1.0 \pm 0.2) \times 10^{-3}$	$(3.2 \pm 1.0) \times 10^{-19}$	$(9.9 \pm 0.2) \times 10^{-4}$	$(3.1 \pm 0.9) \times 10^{-19}$
2H (non-ionizing dissociation)	0.14 ± 0.01	$(4.4 \pm 0.9) \times 10^{-17}$	0.16 ± 0.02	$(5.1 \pm 1.0) \times 10^{-17}$
$H^- + H^+$	$(1.6 \pm 0.3) \times 10^{-3}$	$(5.1 \pm 1.5) \times 10^{-19}$	$(1.5 \pm 0.3) \times 10^{-3}$	$(4.8 \pm 1.4) \times 10^{-19}$
$H^+ + H$	0.29	9.2×10^{-17}	0.31	9.9×10^{-17}
H_2^+ (non-dissociative ionization)	0.50	1.6×10^{-16}	0.48	1.5×10^{-16}
$2H^+$	0.067	2.1×10^{-17}	0.063	2.0×10^{-17}
Total destruction (σ$_{TD}$)	-	$(3.1 \pm 0.5) \times 10^{-16}$	-	$(3.2 \pm 0.5) \times 10^{-16}$
Electron loss °	0.86	2.7×10^{-16}	0.84	2.7×10^{-16}
Sum (H channels)	0.43 ± 0.04	$(1.4 \pm 0.2) \times 10^{-16}$	0.46 ± 0.04	$(1.5 \pm 0.2) \times 10^{-16}$
Sum (H production) [#]	-	$(1.8 \pm 0.3) \times 10^{-16}$	-	$(2.0 \pm 0.3) \times 10^{-16}$
Sum (H^+ channels)	0.36	1.1×10^{-16}	0.37	1.2×10^{-16}
Sum (H^+ production) [#]	-	1.3×10^{-16}	-	1.4×10^{-16}
Total dissociation	0.50 ± 0.04	$(1.6 \pm 0.3) \times 10^{-16}$	0.53 ± 0.04	$(1.7 \pm 0.3) \times 10^{-16}$

Shaded boxes contain branching ratios and cross-sections which were generated by summing distinct channels. [a]Unless errors are specified otherwise. [b]The sum of the $H^+ + H$, H_2^+, and $2H^+$ channels ($\neq$ a current-type electron production cross-section). [c]These cross-sections can be compared directly with current-type measurements, i.e., the cross-sections for channels including the production of two H atoms or two H^+ ions are counted twice for the sums.

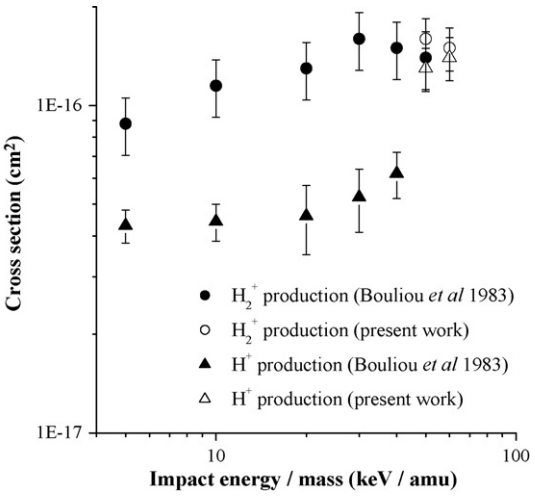

Fig. 7. Comparisons of the present partial cross-sections for H_2^+ and H^+ production in H_2 collisions with helium atoms with the measurements of Bouliou et al. [3].

section (3.0 ± 0.5)[3] $\times 10^{-16}$ cm^2 recommended by Tabata and Shirai [32] for H_2 projectile dissociation in a collision with an H_2 target.

It is interesting to compare the present data with the cross-sections for the ionization and dissociation of H_2 by electron impact reviewed by Tawara et al. [36]. In particular, this review includes cross-sections for specific dissociative electronic excitations determined by the spectroscopic analysis of emitted photons [36]. For 30 eV (1.5 v_0, 56 keV/amu) electron impact upon H_2, cross-section measurements for excitation to the lowest-energy dissociative state, $b^3\Sigma_u^+$, lie in the range $(1–4) \times 10^{-17}$ cm^2 [36]. These results are of the same order as (4.4 ± 0.9) and $(5.1 \pm 1.0) \times 10^{-17}$ cm^2, the present cross-sections for neutral dissociation in helium collisions at 50 and 60 keV/amu, respectively (Table 3). That the present cross-sections are slightly greater than those provided by Tawara et al. [36] is not surprising as the excitation of H_2 into states other than $b^3\Sigma_u^+$ can be expected to contribute to the presently observed non-ionizing dissociation channel.

The present total cross-section $(1.6 \pm 0.3) \times 10^{-16}$ cm^2 for H_2^+ production (non-dissociative ionization) in collisions with He atoms at 50 keV/amu is in agreement with the only directly comparable previous cross-section $(1.4 \pm 0.3) \times 10^{-16}$ cm^2 [3] (see endnote 1). Bouliou et al.'s [3] absolute cross-sections for H^+ and H_2^+ production in H_2 collisions with atomic targets are also in good agreement with earlier measurements in the low-energy part of their range [37,38]. Fig. 7 shows that the present cross-sections are consistent with the broad tendency observed by Bouliou et al. [3] for the H_2^+ production cross-section to increase with impact energy at a steadily decreasing rate for 5–50 keV/amu collisions with He, Ar, and Kr. Indeed, for H_2 impact upon He, no meaningful increase in H_2^+ production between 30 and 50 keV/amu was detected [3]. Accordingly, the present cross-section for H_2^+ production at 60 keV/amu is $(1.5 \pm 0.2) \times 10^{-16}$ cm^2, comfortably within the error margins of the 50 keV/amu result. By contrast, Bouliou et al. [3] observed $d\sigma(H^+)/dE$ as well as $\sigma(H^+)$ to increase with energy in 5–40 keV/amu collisions with He atoms. The present H^+ production cross-sections are $(1.3 \pm 0.2) \times 10^{-16}$ cm^2 at 50 keV/amu and $(1.4 \pm 0.2) \times 10^{-16}$ cm^2 at 60 keV/amu. Thus, while comparison with the previous work [3] may be interpreted to indicate a continued increase in H^+ production up to 50 keV/amu, no evidence is observed in the present data for $\sigma(H^+)$ dependence upon impact energy between 50 and 60 keV/amu. The present cross-sections for H^+ production are ~100% greater than Bouliou et al.'s [3] result at 40 keV/amu, corresponding to a slightly greater increase than would be expected from a simple extrapolation of the previous data.

To the authors' knowledge, the present work provides the first experimental evidence for H^- production in H_2 collisions with an atomic target. Table 3 shows that the sum of the observed H^- production channels ($H^- + H$ and $H^- + H^+$) represents less than 0.3% of H_2 destruction following 50 keV/amu impact upon helium.

Finally, it is interesting to compare the presently observed channels with the potential energy curves corresponding to the electronic states of H_2 and H_2^+ calculated in the Born-Oppenheimer approximation [39]. The observation of non-ionizing dissociation indicates access either to the $b^3\Sigma_u^+$ dissociative state, producing two ground-state H atoms, or to an H_2* state, $B^1\Sigma_u^+$ or $C^1\Pi_u$, which can, with vibrational excitation, lead to the production of two H atoms of which at least one is in an electronic excited state. Excitation to these states from H_2 in the electronic and vibrational ground state requires an energy transfer of several eV up to around 15 eV, depending on the interatomic distance at the instant of excitation, while $2H^+$ production, also observed in the present experiments, requires an energy transfer of around 50 eV. Therefore, the observed channels (Table 3) provide evidence for energy transfer events of several eV to around 50 eV (or greater) in the present impact conditions. This range is consistent with recent energy loss calculations based on a dynamical model for a proton colliding with different atomic targets at energies up to 100 keV [40]. For 50 keV collisions with a weak impact parameter, Cabrera-Trujillo et al. [40] report the kinetic energy lost by the proton and converted into internal energy of the target atom through electronic excitation to be of the order of several tens of eV.

4. Conclusions

This work provides the first absolute cross-section measurements for the various channels of H_3^+ and H_2 dissociation in collisions with helium atoms at 50 and 60 keV/amu. Furthermore, to the authors' knowledge, the present cross-sections

[3] The values given above for the cross sections for H_2 dissociation recommended by Tabata and Shirai [32] are read from a figure as, to our knowledge, the relevant numerical value is not available in the literature. The given error reflects only the precision available from the relevant figure. The value given for Bouliou et al.'s [3] measurement of H_2^+ production in collisions with He atoms at 50 keV/amu has also been taken from a figure. In this case, the error (±20%) is estimated from the error bars on the H^+ production cross-sections presented in the communication.

$(1.6 \pm 0.3) \times 10^{-16}$ and $(1.7 \pm 0.3) \times 10^{-16}$ cm^2 at 50 and 60 keV/amu, respectively, represent the only total dissociation measurements for H_2 in collisions with a helium atom, or indeed any atomic or molecular target at any energy. Comparisons with previous measurements show the present data to be broadly consistent with the trends observed at lower and higher energies. However, it is interesting to note that the present results indicate that electron capture processes contribute more significantly to H^- production in H_3^+ collisions with He at 50 keV/amu than at 0.8–2.3 keV/amu [23]. In addition, comparison of the branching ratios for dissociation following the capture of an electron from a He atom by H_3^+ with those following free electron capture [17] demonstrates major differences, indicating that the helium target has a significant effect on dissociative electron capture processes.

Acknowledgements

Partial financial support was provided by the CNRS, Paris, France, the FWF, Wien, Austria, the French, Austrian, and Morocco governments, the EU Commission (Brussels), in particular through the Amadee and PICS 2290 programs and an FP6 Marie Curie Fellowship (IEF RADAM-BIOCLUS), and the CNRS-CNRST (n°17689) convention. The *Institut de Physique Nucléaire de Lyon* is part of IN2P3-CNRS, the French national research institute for nuclear and particle Physics.

References

[1] T. Oka, Rev. Modern Phys. 64 (1992) 1141.
[2] F. Gobet, B. Farizon, M. Farizon, M.J. Gaillard, J.P. Buchet, M. Carré, T.D. Märk, Phys. Rev. Lett. 89 (2002) 183403;
B. Farizon, M. Farizon, M.J. Gaillard, F. Gobet, M. Carré, J.P. Buchet, P. Scheier, T.D. Märk, Phys. Rev. Lett. 81 (1998) 4108;
S. Eden, J. Tabet, S. Louc, B. Farizon, M. Farizon, S. Ouaskit, T.D. Märk, Phys. Rev. A 73 (2006) 023201.
[3] A. Bouliou, M. Sarret, P. Frere, C. R. Acad. Sci. Paris 296II (1983) 1377.
[4] M. Carré, M. Druetta, M.L. Gaillard, H.H. Bukow, M. Horani, A.L. Roche, M. Velghe, Mol. Phys. 40 (1980) 1453.
[5] M.A. Bolorizadeh, M.E. Rudd, Phys. Rev. A 33 (1986) 893.
[6] S. Ouaskit, B. Farizon-Mazuy, M. Farizon, M.J. Gaillard, E. Gerlic, M. Stern, A. Clouvas, A. Katsanos, Phys. Rev. A 48 (1993) 1204.
[7] S. Ouaskit, B. Farizon, M. Farizon, M.J. Gaillard, E. Gerlic, Phys. Rev. A 49 (1994) 1484.
[8] T.J. Morgan, K.H. Berkner, R.V. Pyle, Phys. Rev. A 5 (1972) 1591.
[9] J.B.A. Mitchell, J.L. Forand, C.T. Ng, D.P. Levac, R.E. Mitchell, P.M. Mul, W. Claeys, A. Sen, J.M. McGowen, Phys. Rev. Lett. 51 (1983) 887.
[10] W. Wolff, L.F.S. Coelho, H.E. Wolf, N.V. de Castro Faria, Phys. Rev. A 45 (1992) 2978.
[11] B. Peart, K.T. Dolder, J. Phys. B 7 (1974) 1567.
[12] Y.K. Bae, M.J. Coggiola, R.J. Peterson, Phys. Rev. A 29 (1984) 2888.
[13] F. Robicheaux, R.P. Wood, C.H. Greene, Phys. Rev. A 49 (1994) 1866.
[14] For example: H. Gnaser, R. Golser, Phys. Rev. A. 73 (2006) 021202.
[15] M.J. Gaillard, A.G. de Pinho, J.C. Poizat, J. Remillieux, R. Saoudi, Phys. Rev. A 28 (1983) 1267.
[16] R. Bruckmeier, Ch. Wunderlich, H. Figger, Phys. Rev. Lett. 72 (1994) 2550.
[17] S. Datz, G. Sundström, C. Biedermann, L. Broström, H. Danared, S. Mannervik, J.R. Mowat, M. Larsson, Phys. Rev. Lett. 74 (1995) 896.
[18] M. Meron, B.M. Johnson, Phys. Rev. A 41 (1990) 1365.
[19] N.V. de Castro Faria, M.J. Gaillard, J.C. Poizat, J. Remillieux, Nucl. Instrum. Methods Phys. Res. B 43 (1989) 1.
[20] G. Jalbert, L.F.S. Coelho, N.V. de Castro Faria, Phys. Rev. A 46 (1992) 3840.
[21] D.L. Montgomery, D.H. Jaecks, Phys. Rev. Lett. 51 (1983) 1862.
[22] I. Alvarez, C. Cisneros, J. de Urquaijo, T.J. Morgan, Phys. Rev. Lett. 53 (1984) 740.
[23] O. Yenen, D.H. Jaecks, L.M. Wiese, Phys. Rev. A 39 (1989) 1767.
[24] L.M. Wiese, O. Yenen, B. Thaden, D.H. Jaecks, Phys. Rev. Lett. 79 (1997) 4982.
[25] G. Hinojosa, F.B. Yousif, C. Cisneros, J. de Urquijo, I. Alvarez, J. Phys. B: Atom. Mol. Opt. Phys. 32 (1999) 915.
[26] J.F. Williams, D. Dunbar, Phys. Rev. 149 (1966) 62.
[27] G.W. McClure, Phys. Rev. 130 (1963) 1852.
[28] W.H. Mais, Phys. Rev. 45 (1934) 773.
[29] E.P. Hunter, S.G. Lias, J. Phys. Chem. Ref. Data 27 (1998) 413.
[30] G. Jalbert, L.F.S. Coelho, N.V. de Castro Faria, Phys. Rev. A 47 (1993) 4768.
[31] J.R. Peterson, P. Devynck, Ch. Hertzler, W.G. Graham, J. Chem. Phys. 96 (1992) 8128.
[32] T. Tabata, T. Shirai, Atom. Data Nucl. Data Tables 76 (2000) 1.
[33] V. Phelps, J. Phys. Chem. Ref. Data 19 (1990) 653.
[34] N.V. de Castro Faria, I. Borges, L.F.S. Coelho, G. Jalbert, Phys. Rev. A 51 (1995) 3831.
[35] E.E. Salpeter, Proc. Phys. Soc. Lond. Sect. A 63 (1950) 1295.
[36] H. Tawara, Y. Itikawa, H. Nishimura, M. Yoshino, J. Phys. Chem. Ref. Data 19 (1990) 617.
[37] E.S. Solov'ev, R.N. Il'in, V.A. Oparin, N.V. Fedorenko, Zh. Eksperim., Soviet Phys., J.E.T.P. 18 (1964) 342.
[38] H.B. Gilbody, R. Browning, Int. Ser. Monogr. Phys. Electr. Ionic Impact Phenom. IV 2964 (1974).
[39] T.E. Sharp, Atom. Data 2 (1971) 119.
[40] R. Cabrera-Trujillo, Y. Öhrn, E. Deumens, J.R. Sabin, Phys. Rev. A 62 (2000) 052714.